nature portfolio

Peer Review File

Subcellular mRNA localization patterns across tissues resolved with spatial transcriptomics

Corresponding Author: Professor Shalev Itzkovitz

This file contains all reviewer reports in order by version, followed by all author rebuttals in order by version.

Version 0:

Reviewer comments:

Reviewer #1

(Remarks to the Author)
SUMMARY

This is an important study by Novoselsky, Golani et al. They developed a user-friendly tool, named HiVis, that uses a robust computational analysis of high-resolution spatial transcriptomic (VisiumHD) data to obtain subcellular mRNA localization patterns in complex mammalian organs/tissues.

They use published and publicly available VisiumHD datasets from normal mouse small intestine and liver, as well as newly generated data from livers.

First, the authors show that HiVis framework is able to accurately reconstruct zonation models of the mouse liver and villi of the small intestine at the single cell level. Reconstructed images of both organs are beautiful and compelling. Then, the authors go deeper into the analysis of subcellular organization of mRNAs within these organs and show convincing evidence of the spatial organization of mRNAs within individual cells in these tissues. Remarkably, the authors found that mRNA localization patterns across organs and species (by comparing mouse and human colon tissue samples) are conserved. The methodology used in this study appears appropriate and properly validated in line with the current gold standard for smFISH imaging technology.

Overall, this is a well-written paper with clear and well-presented data.

This work provides insights into the importance of mRNA localization regulation in normal physiology, a topic that is still understudied, mainly due to technological limitations. Even though computational analysis softwares exist for studying RNA localization patterns in cells in culture, there are no reliable tools for spatial transcriptomic data that provide accurate subcellular resolution to date. The findings of this study are, therefore, significant and will have strong implications in the entire scientific community with great interest not only to RNA scientists and microscopists but also, to cell biologists and pathologists. The use of spatial transcriptomic technologies is currently exponentially growing across all areas of basic and clinical research and tools like the one developed in this work are much needed to pave the way for new discoveries.

There are, however, a few comments detailed below that could be addressed before recommending this manuscript for publication.

MAJOR COMMENTS

Even though this work provides a great resource to study subcellular mRNA localization within intact tissue using spatial transcriptomic data, the authors only focused on two already known mRNA localization patterns in those organs: the apical-basal mRNA localization in gastrointestinal epithelia and nuclear retention in liver hepatocytes. These RNA localization patterns have been elegantly characterized by the Itzkovitz team in the past. I am curious to know if this computational analysis tool could be applied to discover novel RNA localization patterns in tissue beyond the ones described here. If possible, It would present compelling evidence adding to the credibility of the software. If not, it will be appreciated to mention this as a current limitation of the tool.

MINOR COMMENTS

Introduction.
Lines 46/47. The sentence “Computational tools modeling data from imaging-based techniques yielded important insights into subcellular mRNA localization” needs to be referenced. Please, add the proper references, accordingly.

Results
-Development of computational platform for VisiumHD analysis

Line 79. There is no panel “a” in Fig. 1. Please, change the text from ‘Fig. 1a’ to ‘Fig. 1’, accordingly.

Fig. 1. Figure Legend is missing. Please, include the details of the workflow. Even though the schematic is straightforward, the figure will benefit from a brief explanation of every step in the workflow such as the name of the organs, what each drawing/plot represents, what each dot in each volcano plot represents, etc.

-Reconstructing zonation patterns in mouse small intestine and liver using VisiumHD

Line 88. I would suggest changing the title of this section from ‘Reconstructing zonation patterns in mouse small intestine and liver using VisiumHD’ to ‘Reconstructing zonation patterns in mouse small intestine and liver using HiVis’.

Line 107. Please, replace ‘single cell RNA-seq’ with ‘scRNA-seq’, accordingly.

Line 122. Please, mention that hepatocytes are parenchymal cells (PC).

Fig. 3b. Single Cell Segmentation. It would be nice if the upper and bottom panels show the NPC staining. Also, the legend says “NPC”. Since this is an immunofluorescence experiment using antibodies against CD31, I would suggest stating ‘CD31’ in the legend rather than NPC. NPCs can include other cell types such as Kupffer cells. Please, correct this, accordingly.

Figure Legend S3. Line 601/602. ‘In boxplots (c, f-g)’ should be replaced by ‘In boxplots (b, f-g)’

-Polarized mRNA distribution in the intestinal epithelium

Fig. 4a and 4b. It would be appreciated by the reader if the authors can make the color code for apical/basal mRNAs consistent between panels a and b. Apical mRNAs’ title in blue and ‘Basal mRNAs’ title in green. (If they could match the color code used in Fig. 1, it would be nice too!).

Fig. 4c and 4f. The dimensions of the scale bar used are difficult to see. Please, indicate the dimension in the legend as: ‘Scale bar, 10 um’.

Line 172/173 and Fig. 4f and Legend. Is this smFISH or HCR-FISH? Please, make this consistent with the material and methods and correct accordingly.

Fig. S4. The title of this Figure is ‘Mapping nuclear retention across tissues’, however, panels a-c are about polarization in small intestine and human colon. I would suggest splitting this figure: one figure would contain panels a-c titled ‘Mapping apical-basal mRNA polarization across tissues’, and another including panels d-g titled ‘Mapping nuclear retention across tissues.’

Fig. S4b. I would use the same color code for Apical/Basal mRNAs titles to remain consistent with previous figures.

-Specific mRNAs are basally localized in mouse hepatocytes

Fig 5. Could you please use the same color to indicate the sinusoidal cells across all panels?

Fig. 5a. If possible, please, use the same colors for CD31 and DAPI in Fig. 3b.

Fig. 5d. This panel shows central hepatocytes. Do pericentral hepatocytes show the same pattern of localization?

Fig. 5d and 5e. If possible, please, use same color code for apical and basal mRNAs.

Fig. 5f. Line 215 (Legend). Please, change ‘Cyb5r3 (top) and Pigr (bottom)’ to ‘Pigr (top) and Cyb5r3 (bottom)’, accordingly. Also, green arrow and green asterix are difficult to distinguish. Please, make them bigger and show them in different colors.

Could the authors show any newly identified cortical mRNA localization pattern by smFISH? Both examples shown by smFISH are basally polarized mRNAs.

- Mapping nuclear and cytoplasmic mRNA distribution in multiple tissues

Line 226. The sentence “Nuclear-enriched transcripts included Mlxipl, Nlrp6, Sema4g and Pck1 (18)” cites ref 18. However, this is describing the new data provided by this work. Please remove the reference there. Interestingly, Pck1 was not nuclear enriched according to ref 18 and would constitute a case where the RNA localization patterns (nuclear-cytoplasmic) are conflicting. Could the authors explain this discrepancy?

(Remarks on code availability)

Reviewer #2

(Remarks to the Author)
In this manuscript, the authors present HiVis, a computational framework that leverages
High-resolution spatial transcriptomics data to enable subcellular mRNA localization analyses. Overall, this reviewer doesn’t think this work is of significance to the field for the following reasons:

1. HiVis has limited usage given that it only takes VisiumHD data as input. It would be great if it could be compatible with data generated using other spatial transcriptomics technologies such as Stereo-seq, SeqFISH+, MERFISH, and SeqScope.
2. There’s no quantitive evaluation of the cell segmentation results
3. The classification of subcellular compartments seems arbitrary and lacks statistical rigor.
4. It’s unclear what unique advantages HiVis has over existing computational tools such as Ella (https://www.biorxiv.org/content/10.1101/2024.09.23.614515v1.full), Bento (https://link.springer.com/article/10.1186/s13059-024-03217-7), and SPRAWL (https://elifesciences.org/articles/87517).

(Remarks on code availability)
The code provide a README file with enough instructions for installing and running the application

Reviewer #3

(Remarks to the Author)
The manuscript by Novoselsky et al. analyzed public and newly generated VisiumHD data to reveal mRNA localization, especially subcellular apical-basal patterns, in multiple tissues. Their analysis approach is to classify individual 2x2um pixels based on spatial landmarks using the bioimage analysis software QuPath, followed by differential gene expression tests. Their analyses in small intestine and liver suggested conserved apical-basal mRNA localization in different tissue regions.

Major comments:

It may be helpful to describe exactly how the pixel classifiers for subcellular classification were built in detail in the method section. It seems to use the pixel classifier training function in QuPath where the input features possibly contain distance to manually chosen landmarks, but it is unclear from the description of the method.

Giving each pixel a categorical classification seems a major limitation due to both the underlying biology and the data’s property: the subcellular polarization is sometimes a gradient than having a clear boundary, and VisiumHD’s spatial resolution (2x2um) is somewhat limited for high resolution subcellular analysis, some pixels are bound to display apical / basal / nuclear pattern only partially.

The major contribution of the manuscript is the analysis on polarized mRNA distribution, but the relevant analyses come only later in the result section and don’t seem to be elaborated enough. The authors may consider expanding the description of the biology of apical-basal distribution in hepatocytes as it seems the most novel observation. The authors might also emphasize clearly which findings reported in the manuscript are novel, as it may not be very clear to someone not an expert in small intestine or liver.

(Remarks on code availability)

Version 1:

Reviewer comments:

Reviewer #1

(Remarks to the Author)
In the revised version of the manuscript, Novoselsky, Golani et al. have answered most of my concerns and modified the text/figures accordingly. This is now an improved manuscript that provides a wonderful resource that will be valuable for scientists willing to include important subcellular RNA organization analysis to their tissue-scale studies.

I am enthusiastic to recommend this manuscript for immediate publication. At the same time, I would like to encourage the authors to address a few minor remaining points in the text and figures prior to publication.

REMAINING COMMENTS

-Polarized mRNA distribution in the intestinal epithelium – Fig 4.
While highly similar apical-basal RNA localization patterns have been found across mouse small intestine and human colon tissues, a few genes showed a changed in RNA polarization pattern between the two species mouse and human (PMID: 39621797, and this work). While Pigr mRNA was significantly basal in mice (PMID: 39621797 and Fig 4b), PIGR mRNA was significantly apical in humans (PMID: 39621797 and Fig 4e, f). Could the authors briefly acknowledge this change in the polarity between species in the text? PMID: 39621797 could be properly cited here as well.

Line 244. The text says: “Correlation analysis revealed a strong positive agreement with the results of Bahar Halpern et al. (18) (r=0.66, p=3e-103, Fig. 6c), despite major differences in methodology…”. The r=0.66 seems rather a moderate correlation; and I would suggest changing ‘strong positive agreement’ to ‘moderate positive agreement’.

Fig 6 (and Fig 1). I would suggest the authors to color match the nuclear and cytoplasmic enriched mRNAs used in a, d, e and f with mRNA names in MA-plots in panels b, g, h and i in the same way they did for the name of apical/basal mRNAs and titles of MA-plots in previous Figures. The same color code would be appreciated in Fig 1. Currently, the nuclear mRNAs are turquoise and cytoplasmic mRNAs are orange in Fig 6 (a, d, e and f), but the nuclear/cytoplasmic colors are swapped in Fig 1 as well. Also, all mRNA names are in red color in the MA-plots (b, g, h and i). Matching the nuclear/cytoplasmic colors across figure panels would help the reader to visualize faster the main results.

(Remarks on code availability)

Reviewer #2

(Remarks to the Author)
I thank the authors for addressing my previous comments.

In the response to my question about the advantage of HiVis over existing computational methods, the authors stated and I quote, 'HiVis, by contrast, works on binned data generated by sequencing-based methods such as VisiumHD, Stereo-seq, and Slide-seq, thereby leveraging whole-transcriptome measurements.' However, I did not see examples of the applications of HiVis in Stereo-seq and Slide-seq datasets. I would like to see these demonstrations to be fully convinced that HiVis is a generalizable tool rather than a tool built for just Visium data.

(Remarks on code availability)

Reviewer #3

(Remarks to the Author)
Although the authors made an effort to show that the users can import data from high resolution platforms (MERFISH, Xenium datasets), there is no enough evidence that the tool can analyze those data effectively, especially given that there are existing tools to visualize those data much more efficiently. The additional figure only shows that the tool can display the raw image and very low resolution summary of the transcripts, saying that it is now compatible with multiple platforms is not justified. It is better to acknowledge that it is specialized to Visium HD (which is fine since Visium HD has many properties distinct from imaging based platforms).

(Remarks on code availability)

Version 2:

Reviewer comments:

Reviewer #1

(Remarks to the Author)
The authors have answered all my concerns. I recommend this manuscript for publication.

(Remarks on code availability)

Reviewer #2

(Remarks to the Author)
The authors have now addressed all my comments. The manuscript is suitable for publication.

(Remarks on code availability)

Reviewer #3

(Remarks to the Author)

(Remarks on code availability)

Reviewer #1:

SUMMARY

This is an important study by Novoselsky, Golani et al. They developed a user-friendly tool, named HiVis, that uses a robust computational analysis of high-resolution spatial transcriptomic (VisiumHD) data to obtain subcellular mRNA localization patterns in complex mammalian organs/tissues.

They use published and publicly available VisiumHD datasets from normal mouse small intestine and liver, as well as newly generated data from livers.

First, the authors show that HiVis framework is able to accurately reconstruct zonation models of the mouse liver and villi of the small intestine at the single cell level. Reconstructed images of both organs are beautiful and compelling. Then, the authors go deeper into the analysis of subcellular organization of mRNAs within these organs and show convincing evidence of the spatial organization of mRNAs within individual cells in these tissues. Remarkably, the authors found that mRNA localization patterns across organs and species (by comparing mouse and human colon tissue samples) are conserved. The methodology used in this study appears appropriate and properly validated in line with the current gold standard for smFISH imaging technology.

Overall, this is a well-written paper with clear and well-presented data.

This work provides insights into the importance of mRNA localization regulation in normal physiology, a topic that is still understudied, mainly due to technological limitations. Even though computational analysis softwares exist for studying RNA localization patterns in cells in culture, there are no reliable tools for spatial transcriptomic data that provide accurate subcellular resolution to date. The findings of this study are, therefore, significant and will have strong implications in the entire scientific community with great interest not only to RNA scientists and microscopists but also, to cell biologists and pathologists. The use of spatial transcriptomic technologies is currently exponentially growing across all areas of basic and clinical research and tools like the one developed in this work are much needed to pave the way for new discoveries.

There are, however, a few comments detailed below that could be addressed before recommending this manuscript for publication.

MAJOR COMMENTS

Even though this work provides a great resource to study subcellular mRNA localization within intact tissue using spatial transcriptomic data, the authors only focused on two already known mRNA localization patterns in those organs: the apical-basal mRNA localization in gastrointestinal epithelia and nuclear retention in liver hepatocytes. These RNA localization patterns have been elegantly characterized by the Itzkovitz team in the past. I am curious to know if this computational analysis tool could be applied to discover novel RNA localization patterns in tissue beyond the ones described here. If possible, it would present compelling evidence adding to the credibility of the software. If not, it will be appreciated to mention this as a current limitation of the tool.

We thank the reviewer for this comment. Indeed, our lab has previously described the apical-basal polarization in the mouse and human intestinal epithelium. However, mRNA subcellular polarization in the liver cannot be resolved using LCM-based methods due to the non-linear compartments and the need for associated image-processing of membrane and vessel staining. In our current manuscript, we utilized VisiumHD, together with appropriate tissue staining to extract, for the first time, basal mRNA polarization in hepatocytes. We now stress the novelty of this in our manuscript on page 13:

"Unlike the intestinal epithelium, the distinct morphology of hepatic plates complicates the characterization of apical–basal mRNA polarization in the liver. In this study, we combined membrane and endothelial staining with high-resolution spatial transcriptomics to identify, for the first time, a small set of hepatocyte transcripts exhibiting basal polarization."

To further demonstrate the utility of our approach to uncover new polarization patterns, we have now performed a new analysis that quantifies the extent of the mRNA apical polarization. To this end, we defined two apical sub-compartments – a perinuclear compartment closer to the nucleus, and a luminal compartment closer to the luminal surface of the cells. Importantly, these sub-compartments were extracted automatically using our software and the nuclear and cellular segmentations. We identified genes that show different polarization patterns within the apical compartment, and validated two of them with smFISH – Lct and Atp1b1. These results are presented on page 8:

“We further examined whether apically localized transcripts exhibit preferential luminal versus perinuclear enrichment (Fig. S4c–d) and observed clear differences between these patterns (Supplementary Table 2). For example, Lct showed strong luminal apical localization, whereas Atp1b1 displayed a more uniformly distributed apical pattern (Fig. S4e–g).”

And in the new Fig. S4c-g:

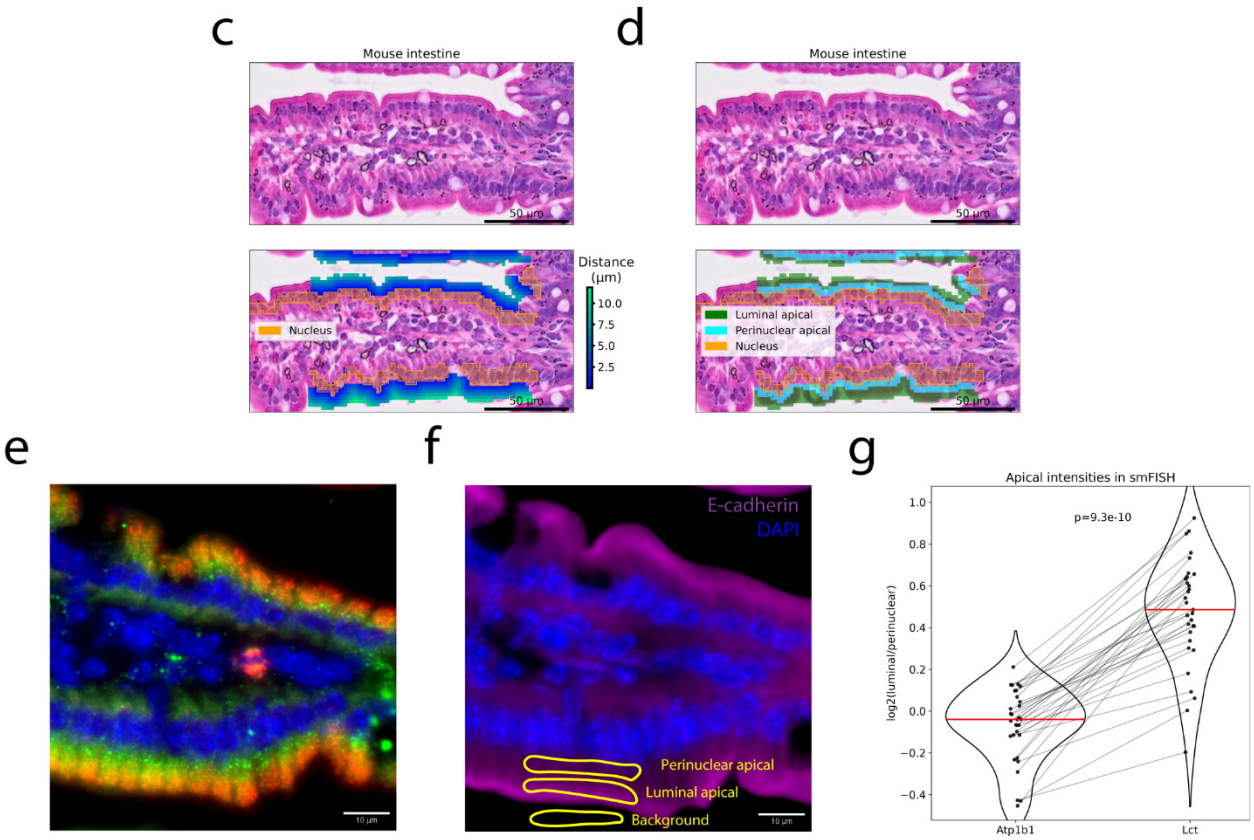

(c) *Mouse proximal intestine VisiumHD H&E image (top) and overlayed with 2×2µm bins colored by the distance to the nuclei (bottom).* ***(d)*** *Mouse proximal intestine VisiumHD H&E image (top) and overlayed with 2×2µm bins colored by apical sub-compartments (bottom).* ***(e)*** *smFISH staining of Lct and Atp1b1 in mouse proximal intestine. Image is representative of 2 mice. Scale bar, 10 µm.* ***(f)*** *Example annotation of apical sub-compartments and background, used for quantification of smFISH intensity. Annotations are based on Immunofluorescence staining of E-cadherin and nuclei. Same FOV as (e).* ***(g)*** *Quantification of apical smFISH signal as log2(luminal/perinuclear) intensity for Atp1b1 and Lct. Lines connect paired measurements across annotated apical sub-compartments. Red lines indicate medians. p-value calculated by Wilcoxon signed-rank test. Annotations are from two mice.*

MINOR COMMENTS

Lines 46/47. The sentence “Computational tools modeling data from imaging-based techniques yielded important insights into subcellular mRNA localization” needs to be referenced. Please, add the proper references, accordingly.

We have added proper references for the sentence.

-Development of computational platform for VisiumHD analysis

Line 79. There is no panel “a” in Fig. 1. Please, change the text from ‘Fig. 1a’ to ‘Fig. 1’, accordingly.

We removed “a” from “1a”.

Fig. 1. Figure Legend is missing. Please, include the details of the workflow. Even though the schematic is straightforward, the figure will benefit from a brief explanation of every step in the workflow such as the name of the organs, what each drawing/plot represents, what each dot in each volcano plot represents, etc.

We thank the reviewer for noting this, we have now added a legend for the figure:

“**Figure 1 – Workflow for detection of subcellular mRNA localization using HiVis**. *Analysis workflow for VisiumHD datasets. Images are segmented into single cells, tissue and cell type specific information is incorporated to enable precise subcellular analyses. Apical–basal and nuclear–cytoplasmic compartments are assigned to spatial bins, and differential gene expression analysis is performed to identify genes localized to these compartments. Validation is carried out using in-situ hybridization stainings.*”

-Reconstructing zonation patterns in mouse small intestine and liver using VisiumHD

Line 88. I would suggest changing the title of this section from ‘Reconstructing zonation patterns in mouse small intestine and liver using VisiumHD’ to ‘Reconstructing zonation patterns in mouse small intestine and liver using HiVis’.

We have made the suggested change.

Line 107. Please, replace ‘single cell RNA-seq’ with ‘scRNA-seq’, accordingly.

We have made the suggested change.

Line 122. Please, mention that hepatocytes are parenchymal cells (PC).

We have made the suggested change.

Fig. 3b. Single Cell Segmentation. It would be nice if the upper and bottom panels show the NPC staining. Also, the legend says "NPC". Since this is an immunofluorescence experiment using antibodies against CD31, I would suggest stating 'CD31' in the legend rather than NPC. NPCs can include other cell types such as Kupffer cells. Please, correct this, accordingly.

The "NPC" labeled regions in Fig. 3b are not the CD31 staining, rather, these are segmented NPCs (can indeed also be Kupffer cells rather than endothelial cells) within the sinusoidal compartment that was identified using CD31 and ATP1A1. We now describe this in the figure caption:

"*NPC – non parenchymal cells, residing in the sinusoids, which are segmented based on CD31 and ATP1A1 staining (Methods).*"

And in the Methods section on page 19:

"*NPCs were segmented within blood vessel regions using an in-house–trained StarDist model on the DAPI channel, with expansion restricted to vessel regions and capped at 2 µm. The StarDist threshold was set to 0.3 with normalization percentiles of 1 and 99. NPC were further filtered by size (nuclear area 10-80 µm^2) and by DAPI intensity >18,000.*"

Figure Legend S3. Line 601/602. 'In boxplots (c, f-g)' should be replaced by 'In boxplots (b, f-g)'

We updated the legend accordingly.

-Polarized mRNA distribution in the intestinal epithelium

Fig. 4a and 4b. It would be appreciated by the reader if the authors can make the color code for apical/basal mRNAs consistent between panels a and b. Apical mRNAs' title in blue and 'Basal mRNAs' title in green. (If they could match the color code used in Fig. 1, it would be nice too!).

We have updated the colors to match Fig. 1. We also updated Fig. 4e and Fig. S4 accordingly.

Fig. 4c and 4f. The dimensions of the scale bar used are difficult to see. Please, indicate the dimension in the legend as: 'Scale bar, 10 um'.

We updated the legend accordingly.

Line 172/173 and Fig. 4f and Legend. Is this smFISH or HCR-FISH? Please, make this consistent with the material and methods and correct accordingly.

We have now updated all instances of smFISH in the text, where HCR was used. We have also split the methods section for both methods.

Fig. S4. The title of this Figure is 'Mapping nuclear retention across tissues', however, panels a-c are about polarization in small intestine and human colon. I would suggest splitting this figure: one figure would contain panels a-c titled 'Mapping apical-basal mRNA polarization across tissues', and another including panels d-g titled 'Mapping nuclear retention across tissues.'

We have now split the figure into two, as suggested, one focusing on apical-basal polarization in the colon and across tissues (Figure S4), and the second focusing on nuclear retention in livers of human and mouse and across tissues (Figure S5).

Fig. S4b. I would use the same color code for Apical/Basal mRNAs titles to remain consistent with previous figures.

We have modified the colors as in Figs. 1, 4, 5.

-Specific mRNAs are basally localized in mouse hepatocytes

Fig 5. Could you please use the same color to indicate the sinusoidal cells across all panels?

We have modified the colors as suggested.

Fig. 5a. If possible, please, use the same colors for CD31 and DAPI in Fig. 3b.

We have modified the colors in Fig. 3b to match those in Fig. 5a.

Fig. 5d. This panel shows central hepatocytes. Do pericentral hepatocytes show the same pattern of localization?

We apologize for the confusion, the meaning of 'central' in Fig. 5d pertained to the centers of the cells rather than to pericentral or mid-lobular hepatocytes. Rather, all hepatocytes were included in this analysis. We have now renamed this category to "core" to avoid misinterpretation.

Regarding polarization in different lobule zones, we attempted to address this in our analysis, but unfortunately, zone-dependent apical–basal quantification lacked sufficient statistical power, so we did not include these results in the figures. Based on the smFISH images, both Cyb5r3 and Pigr exhibit basal localization across hepatic zones.

Fig. 5d and 5e. If possible, please, use same color code for apical and basal mRNAs.

We have modified the colors as in Fig. 1, 4, S4.

Fig. 5f. Line 215 (Legend). Please, change 'Cyb5r3 (top) and Pigr (bottom)' to 'Pigr (top) and Cyb5r3 (bottom)', accordingly. Also, green arrow and green asterix are difficult to distinguish. Please, make them bigger and show them in different colors. Could the authors show any newly identified cortical mRNA localization pattern by smFISH? Both examples shown by smFISH are basally polarized mRNAs.

We have now updated the legend and the figure. We have also attempted to validate four of the cortical genes, however, unfortunately the HCR probe design failed on three of these and the remaining one had issues with non-specific binding. We therefore did not include any discussion of potential cortical genes in the manuscript (unlike the basal genes Pigr and Cyb5r3 which we had validated).

- Mapping nuclear and cytoplasmic mRNA distribution in multiple tissues

Line 226. The sentence "Nuclear-enriched transcripts included Mlxipl, Nlrp6, Sema4g and Pck1 (18)" cites ref 18. However, this is describing the new data provided by this work. Please remove the reference there. Interestingly, Pck1 was not nuclear enriched according to ref 18

and would constitute a case where the RNA localization patterns (nuclear-cytoplasmic) are conflicting. Could the authors explain this discrepancy?

We have removed the reference from the sentence, as suggested. Regarding Pck1, it is correct that this gene was not reported as nuclear retained in ref. 18. The numbers of mRNA molecules in the nucleus for Pck1 is around $\frac{1}{4}$ of the number in the cytoplasm. This is still higher than other genes such as Actb, where the number of nuclear transcripts is $\frac{1}{40}$ of those in the cytoplasm. Beyond relatively high levels in the nucleus, Pck1 transcripts show perinuclear localization (PMID 25728770), which may lead our method to classify it as nuclear-enriched. We have now added a note in the Discussion to clarify this potential limitation on page 13:

"*Sequencing-based spatial transcriptomics, in contrast, is highly scalable and continues to improve, though it remains constrained by molecular diffusion and spatial resolution. For example, the 2 µm resolution of VisiumHD can blur adjacent subcellular regions, causing perinuclear cytoplasmic transcripts to be misclassified as nuclear. Its major advantages include unbiased whole-transcriptome coverage and compatibility with FFPE samples, enabling exploratory analyses of archival and diseased tissues under diverse conditions.*"

Reviewer #2:

In this manuscript, the authors present HiVis, a computational framework that leverages High-resolution spatial transcriptomics data to enable subcellular mRNA localization analyses. Overall, this reviewer doesn't think this work is of significance to the field for the following reasons:

1. HiVis has limited usage given that it only takes VisiumHD data as input. It would be great if it could be compatible with data generated using other spatial transcriptomics technologies such as Stereo-seq, SeqFISH+, MERFISH, and SeqScope.

We thank the reviewer for this suggestion. Although HiVis was developed and primarily tested on VisiumHD datasets, the framework is platform agnostic. We have now expanded the tool to more flexibly support additional spatial transcriptomics platforms. HiVis now accepts any dataset that provides an image, a binned expression matrix, and corresponding spatial coordinates, making it compatible with a wide range of technologies beyond VisiumHD. For imaging-based platforms that produce single-molecule coordinates (e.g., MERFISH, SeqFISH+, Xenium), these coordinates can be readily aggregated into spatial bins prior to import.
We have also implemented dedicated functions for importing raw MERFISH and XENIUM data. We have added usage examples for working with these datasets to the code repository linked in the paper (https://github.com/roynov01/HiVis). As examples, we imported, visualized, and analyzed a MERFISH dataset of human liver (Yakubovsky et al., 2025) and XENIUM data from human ductal adenocarcinoma (10x Genomics, https://www.10xgenomics.com/datasets/ffpe-human-ductal-adenocarcinoma-data-with-human-immuno-oncology-profiling-panel-1-standard):

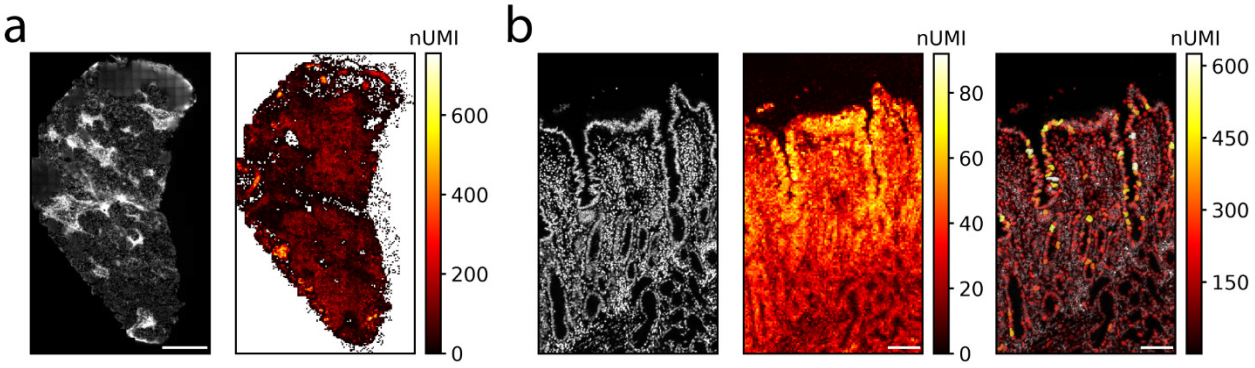

Fig. R1 – Demonstrating the compatibility of HiVis with MERFISH and XENIUM datasets.
a. *MERFISH dataset of healthy human liver (Yakubovsky et al. 2025), imported, analyzed and visualized using HiVis. left: DAPI staining. Right: the same ROI with transcripts aggregated into 30 µm bins, colored by UMI count. Scale bar 1 mm.*
b. *XENIUM dataset of human ductal adenocarcinoma (10x Genomics) imported, analyzed and visualized using HiVis. Left: DAPI staining. Middle: the same ROI with transcripts aggregated into 6 µm bins, colored by UMI count. Right: the same ROI, with 6 µm bins aggregated into single cells, colored by UMI count. Single-cell segmentation was performed in QuPath. Scale bar 100µm.*

We now mention the compatibility of HiVis with those platforms in the text, on page 3:
"To address this gap, we developed HiVis (HD Integrated Visium Interactive Suite), an interactive, user-friendly, end-to-end platform optimized for 10x VisiumHD datasets but extended to support other spatial transcriptomics methods (Fig. S1)."

We have also updated the abstract to highlight the ability of our tool to analyze high-definition spatial transcriptomics rather than specifically VisiumHD.

2. There's no quantitative evaluation of the cell segmentation results

We thank the reviewer for this comment. In response, we performed an extensive evaluation of our custom-trained Cellpose model for cell segmentation. The model showed substantially improved performance compared with the default Cellpose *cyto3* model as well as a StarDist-based approach with expansion. Overall, our model achieved an object-level F1 score of 0.87 and an Aggregated Jaccard Index of 0.73, with a precision of 0.92 and a recall of 0.83. We have added the complete quantitative evaluation results to Supplementary Table 3. We have also added a description of the evaluation in the methods section on page 19:

"Segmentation performance was evaluated by selecting an additional 20 regions (10 from each sample) and manually segmenting ~80 cells per region, defined as a ground truth (GT) dataset. Our applied custom Cellpose model was compared against the built-in cyto3 Cellpose model – both based on membrane and nuclei signals – and against nuclei segmentation with expansion approach using Stardist and Cellpose (Supplementary Table 3). To assess segmentation performance an intersection-over-union (IoU) was computed for each pair of matching cells. IoU was computed as the number of intersecting pixels between the two segmented objects divided by the union of the pixels of the two objects. A correct match was considered only if IoU was larger than 0.5, namely if the overlap between the GT and the segmented cell encompassed more than 50% of the pixels in the union of both objects. Following this calculation, commonly used precision metrics were computed, including recall, F1 score Aggregated Jaccard Index (AJI):

$$Object\ F1 = \frac{2 \cdot TP}{2 \cdot TP + FP + FN}$$

$$Average\ precision = \frac{TP}{TP + FP + FN}$$

$$Object\ precision = \frac{TP}{TP + FP}$$

$$Object\ recall = \frac{TP}{TP + FN}$$

$$Aggregated\ Jaccard\ Index\ (AJI) = \frac{\sum |\ GT_i \cap Pred_j\ |}{\sum |\ GT_i \cap Pred_j\ | + unmatched\ areas}$$

Where TP denotes true positive detections, defined as one-to-one matches between ground truth (GT) objects, and predictions with an IoU ≥ 0.5. FP denotes false positive detections (predicted objects not matched to any GT object), and FN denotes false negatives (GT objects without a corresponding prediction). AJI computes the sum over all matched pairs of their overlapping pixels divided by this sum and the total sum of areas that are unmatched (both non-overlapping pixels in matched pairs and total pixels of unmatched objects and GT)."

For other tissues, cell segmentation was intentionally performed using nuclear detection followed by controlled expansion, rather than full membrane-based segmentation. In these tissues, reliable membrane markers were not available, making precise delineation of cell boundaries inherently ambiguous. We therefore adopted a conservative nucleus-based approximation in which the cytoplasm was defined as a rim around the nucleus (in the human liver) or based on nuclear/cytoplasmic pixel classification (in the human colon and mouse jejunum). This is sufficient for the

nuclear–cytoplasmic differential expression analyses presented in this manuscript. In addition, all apical–basal analyses in the intestinal tissues were performed using a pixel classifiers rather than cell-level segmentation, further reducing dependence on precise cell boundary delineation.

3. The classification of subcellular compartments seems arbitrary and lacks statistical rigor.

We thank the reviewer for this comment. Unlike in the liver dataset – where subcellular compartments can be precisely delineated using fluorescent membrane staining and sinusoidal detection – the apical–basal classification in the intestine relied on a pixel classifier trained on manual annotations. To validate this approach, we repeated the analysis using manually segmented apical and basal compartments, following the strategy used in previous LCM-based studies of apical–basal mRNA polarization (https://www.science.org/doi/10.1126/science.aan2399, https://journals.plos.org/plosbiology/article?id=10.1371/journal.pbio.3002942).
We observe a highly significant positive correlation between the manually derived compartment labels and the pixel-classifier output (Fig. S4a), demonstrating that the classifier provides a robust and biologically meaningful representation of apical–basal localization:

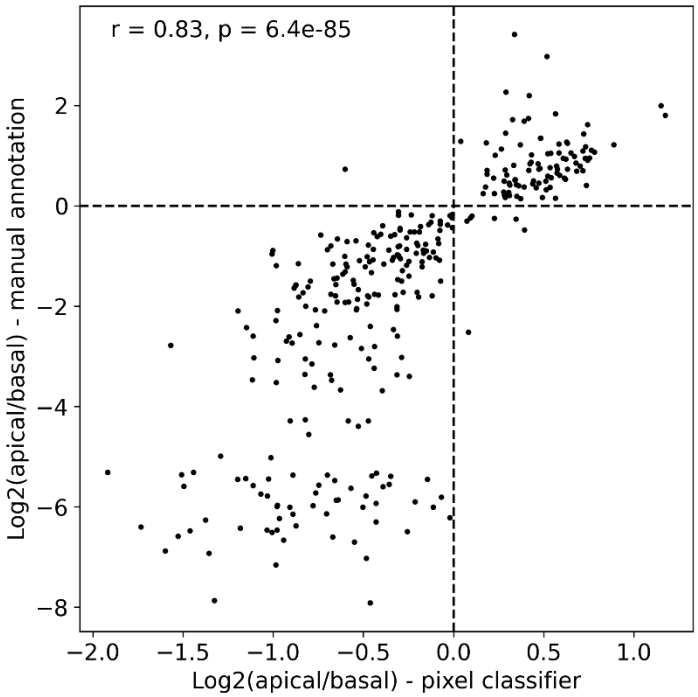

Fig. S4a – Spearman correlation of apical-basal bias in mouse proximal small intestine using manual annotation and pixel classifier. Genes with normalized expression > 10^{-5} and q<0.05 are used.

This validation is described on page 8:
"The apical-basal enrichment patterns obtained with pixel classifier were consistent with those derived from manual annotations (r=0.83, p=6e-85, Fig S4a)."

4. It's unclear what unique advantages HiVis has over existing computational tools such as Ella (https://www.biorxiv.org/content/10.1101/2024.09.23.614515v1.full), Bento (https://link.springer.com/article/10.1186/s13059-024-03217-7), and SPRAWL (https://elifesciences.org/articles/87517).

We thank the reviewer for the comment. The specified tools are indeed highly effective for identifying subcellular localization. HiVis differs from these frameworks in several aspects:

1. **Compatibility with sequencing-based spatial transcriptomics. The existing tools operate on imaging-based spatial transcriptomics data, which rely on single-molecule coordinates from platforms such as MERFISH, CosMx, SeqFISH, and Xenium. Although these approaches offer high spatial resolution, they are limited in the number of genes that can be targeted, and their library design is technically demanding, often requiring careful selection of genes that are not overly abundant, among other constraints. HiVis, by contrast, works on binned data generated by sequencing-based methods such as VisiumHD, Stereo-seq, and Slide-seq, thereby leveraging whole-transcriptome measurements. As noted above, the tool is designed to be flexible and can also be applied to imaging-based datasets, if transcript coordinates are first aggregated into bins.**
2. **Independence from single-cell masks. Ella, Bento, and SPRAWL rely on single-cell masks for subcellular analysis, whereas HiVis operates at the bin level, enabling analyses that does not depend on accurate cell segmentation. This is particularly useful in settings where high-quality segmentation is not achievable. For example, this is the case for the mouse small intestine, human colon and human liver datasets in our manuscript, which include only H&E staining, where apical, basal, and nuclear regions can still be compared even without precise delineation of individual cells, especially along the lateral membrane.**
3. **Explicit modeling of in-tissue context. A key distinction between Ella, Bento, SPRAWL, and HiVis is the isolated-cell versus in-tissue analysis. While these tools robustly detect subcellular localization patterns by applying statistical**

tests to individual cell masks, HiVis retains each cell's spatial context within the tissue and incorporates image-derived information. This enables the identification of tissue-dependent "peripheral" compartments and polarity features. For example, apical and basal domains in intestinal epithelia would both appear as generic peripheral regions when analyzed solely through cell masks, whereas incorporating the tissue context allows these domains to be assigned using pixel classification or by computing the distance to the lumen. Likewise, basal compartments in liver hepatocytes can only be recognized through proximity to sinusoids, a feature that requires tissue-level context. By integrating imaging information with segmentation when available, HiVis enables analyses that would not be possible when relying exclusively on isolated cell masks.

4. **Multi-scale integration across tissue, regions, cells, and subcellular compartments. Related to point (3), HiVis supports integrated analysis across bins, cells, anatomical regions, and tissue-level contexts within a single framework. This flexibility allowed us to investigate spatial zonation in both the intestine and liver. While such analyses could, in principle, be performed using other tools, HiVis implements all steps in a unified and reproducible pipeline. For instance, our small intestine workflow combines manual annotation of anatomical regions (e.g., individual villi), cell segmentation, single-cell analysis within spatial context (including cell-type assignment and distance to the muscle layer), and subsequent subcellular analysis that builds directly on these intermediate results.**

We have now clarified these unique advantages of HiVis in the discussion on page 13:
"*To enable these analyses, we developed HiVis, a flexible tool that streamlines analysis across diverse datasets by integrating image processing tools, tissue-specific single-cell segmentation, customized workflows, and subcellular transcript-localization analyses. In contrast to existing frameworks for subcellular transcriptomics, such as SPRAWL (28), Bento (29) and Ella (30), HiVis does not rely on isolated single-cell masks as the primary spatial unit. Instead, it integrates image-derived tissue context with segmentation outputs, allowing polarity features that depend on anatomical structure – such as lumen proximity in the intestine or sinusoidal orientation in the liver – to be captured. HiVis can also analyze binned spatial data when segmentation is incomplete, while still supporting full mask-based workflows when high-quality masks are available. Together, these features provide a unified framework for linking anatomical annotation, spatial zonation, and subcellular localization.*"

Remarks on code availability:

The code provides a README file with enough instructions for installing and running the application

Reviewer #3:

The manuscript by Novoselsky et al. analyzed public and newly generated VisiumHD data to reveal mRNA localization, especially subcellular apical-basal patterns, in multiple tissues. Their analysis approach is to classify individual 2x2um pixels based on spatial landmarks using the bioimage analysis software QuPath, followed by differential gene expression tests. Their analyses in small intestine and liver suggested conserved apical-basal mRNA localization in different tissue regions.

Major comments:

1. It may be helpful to describe exactly how the pixel classifiers for subcellular classification were built in detail in the method section. It seems to use the pixel classifier training function in QuPath where the input features possibly contain distance to manually chosen landmarks, but it is unclear from the description of the method.

We thank the reviewer for pointing this out. The pixel classifiers do not rely on manually defined landmarks. Instead, they are trained directly on image-derived features provided by QuPath's pixel-classifier framework. These include multiscale intensity-, edge-, curvature-, and texture-based features across all available channels. We have now added this clarification to the Methods section (page 16):

"Pixel classifiers in Qupath were trained using user-annotated examples for each class and relied solely on QuPath's built-in multiscale image features; No manually defined landmarks or distance-based features were used."

2. Giving each pixel a categorical classification seems a major limitation due to both the underlying biology and the data's property: the subcellular polarization is sometimes a gradient than having a clear boundary, and VisiumHD's spatial resolution (2x2um) is somewhat limited for high resolution subcellular analysis, some pixels are bound to display apical / basal / nuclear pattern only partially.

VisiumHD bins (2 × 2 µm) indeed contain multiple underlying image pixels, and subcellular polarization can occur along a continuum rather than at sharp boundaries. In principle, QuPath's pixel classifier can be applied at full image resolution, allowing each bin to be represented by class proportions rather than a single categorical label. However, in our experience, operating at very fine resolution introduces substantial

noise, particularly in H&E or low-contrast channels. For this reason, all pixel classifiers in the present study were trained at a moderate resolution close to the 2 µm bin size, resulting in one class assignment per bin.

Nevertheless, HiVis fully supports proportion-based representations, where each bin receives the percentage of pixels assigned to each class. This enables gradient-like patterns to be modeled when image quality and signal allow, and we highlight this as an analysis option in the documentation (https://github.com/roynov01/HiVis/tree/main/QuPath).

3. The major contribution of the manuscript is the analysis on polarized mRNA distribution, but the relevant analyses come only later in the result section and don't seem to be elaborated enough. The authors may consider expanding the description of the biology of apical-basal distribution in hepatocytes as it seems the most novel observation. The authors might also emphasize clearly which findings reported in the manuscript are novel, as it may not be very clear to someone not an expert in small intestine or liver.

We have now added a dedicated paragraph in the Results section that provides additional biological context on hepatocyte polarity, outlines what is known, and highlights the existing gaps. We also explicitly state that our study provides the first demonstration of cytoplasmic mRNA polarization in hepatocytes *(page 10):*

"Hepatocytes in the mammalian liver are arranged in radial sheets that span the portal-central axis. Each hepatocyte has two basal sides, facing the sinusoidal blood vessels, and cortical sides that face adjacent hepatocytes (these include the apical sides that face the bile canaliculi) (54). In this case, apical and basal domains are not easily identifiable and therefore cannot be reliably isolated by LCM. As a result, mRNA localization to these compartments has remained uncharacterized, making it an ideal test case for our approach."

"Differential gene expression analysis identified several basally enriched transcripts, including Scd1, Pigr, Cald1, and Cyb5r3 (Fig. 5e, Supplementary table 2). Validation by smFISH confirmed basal localization of Pigr and Cyb5r3 (Fig. 5f), providing, to our knowledge, the first evidence of cytoplasmic mRNA polarization in hepatocytes."

Similarly, we added a sentence emphasizing the novelty of the results in the apical-basal polarization in the human colon (page 8):

"Together, these results demonstrate that colon epithelial cells exhibit clear apical–basal mRNA polarization, extending this localization pattern to an additional region of the gastrointestinal tract."

And in nuclear-cytoplasmic mapping across the tissues (page 11):

"High-throughput mapping of nuclear–cytoplasmic mRNA localization has previously been explored in the mouse liver, yet not in the gastrointestinal tract nor in human. Therefore, we extended our analysis to additional tissues, including mouse proximal small intestine (Fig. 6d), human colon (Fig. 6e), as well as a recently published human liver dataset from a live organ donor (44) (Fig. 6f, S5b). While performed only in mouse liver, comparable analyses have not been carried out in these tissues."

To further demonstrate the utility of our approach to uncover new polarization patterns, in the revised manuscript, we have now performed a new analysis that quantifies the extent of the mRNA apical polarization (a polarization pattern not explored to date in tissues). To this end, we defined two apical sub-compartments – a perinuclear compartment closer to the nucleus, and a luminal compartment closer to the luminal surface of the cells. Importantly, these sub-compartments were extracted automatically using our software and the nuclear and cellular segmentations. We identified genes that show different polarization patterns within the apical compartment, and validated two of them with smFISH – Lct and Atp1b1. These results are presented on page 8:

"We further examined whether apically localized transcripts exhibit preferential luminal versus perinuclear enrichment (Fig. S4c–d) and observed clear differences between these patterns (Supplementary Table 2). For example, Lct showed strong luminal apical localization, whereas Atp1b1 displayed a more uniformly distributed apical pattern (Fig. S4e–g)."

And in the new Fig. S4c-g:

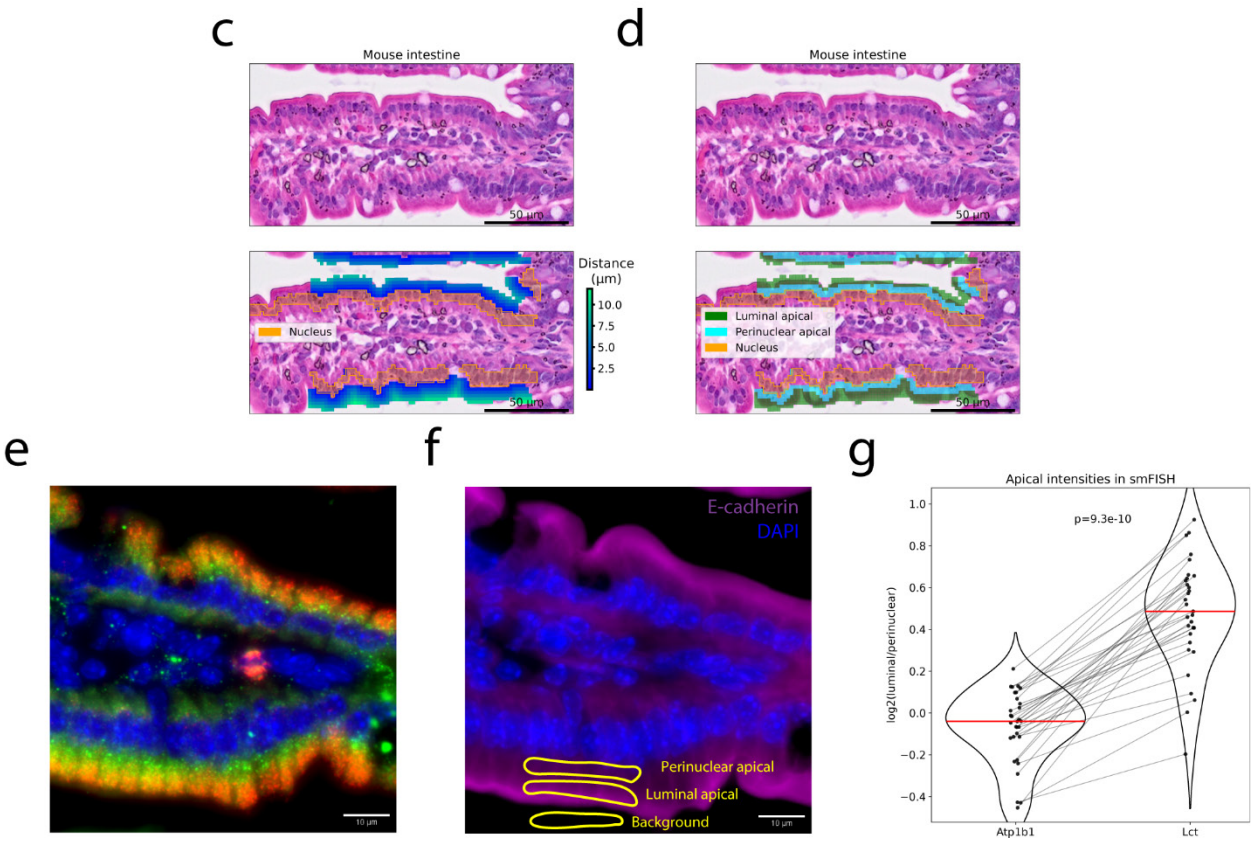

(c) *Mouse proximal intestine VisiumHD H&E image (top) and overlayed with 2×2µm bins colored by the distance to the nuclei (bottom).* ***(d)*** *Mouse proximal intestine VisiumHD H&E image (top) and overlayed with 2×2µm bins colored by apical sub-compartments (bottom).* ***(e)*** *smFISH staining of Lct and Atp1b1 in mouse proximal intestine. Image is representative of 2 mice. Scale bar, 10 µm.* ***(f)*** *Example annotation of apical sub-compartments and background, used for quantification of smFISH intensity. Annotations are based on Immunofluorescence staining of E-cadherin and nuclei. Same FOV as (e).* ***(g)*** *Quantification of apical smFISH signal as log2(luminal/perinuclear) intensity for Atp1b1 and Lct. Lines connect paired measurements across annotated apical sub-compartments. Red lines indicate medians. p-value calculated by Wilcoxon signed-rank test. Annotations are from two mice.*

Response to referees

Reviewer #1:

In the revised version of the manuscript, Novoselsky, Golani et al. have answered most of my concerns and modified the text/figures accordingly. This is now an improved manuscript that provides a wonderful resource that will be valuable for scientists willing to include important subcellular RNA organization analysis to their tissue-scale studies.

I am enthusiastic to recommend this manuscript for immediate publication. At the same time, I would like to encourage the authors to address a few minor remaining points in the text and figures prior to publication.

REMAINING COMMENTS

-Polarized mRNA distribution in the intestinal epithelium – Fig 4. While highly similar apical-basal RNA localization patterns have been found across mouse small intestine and human colon tissues, a few genes showed a changed in RNA polarization pattern between the two species mouse and human (PMID: 39621797, and this work). While Pigr mRNA was significantly basal in mice (PMID: 39621797 and Fig 4b), PIGR mRNA was significantly apical in humans (PMID: 39621797 and Fig 4e, f). Could the authors briefly acknowledge this change in the polarity between species in the text? PMID: 39621797 could be properly cited here as well.

We thank the reviewer for the comments. We have now added a note of this discrepancy in the results section on page 8 and added this highly relevant reference:

"As shown in previous work (14), PIGR exhibited significant apical localization in humans, and significant basal localization in mice (Fig. 4b, e, f)."

Line 244. The text says: "Correlation analysis revealed a strong positive agreement with the results of Bahar Halpern et al. (18) (r=0.66, p=3e-103, Fig. 6c), despite major differences in methodology…". The r=0.66 seems rather a moderate correlation; and I would suggest changing 'strong positive agreement' to 'moderate positive agreement'.

We have made the suggested change.

Fig 6 (and Fig 1). I would suggest the authors to color match the nuclear and cytoplasmic enriched mRNAs used in a, d, e and f with mRNA names in MA-plots in panels b, g, h and i in the same way they did for the name of apical/basal mRNAs and titles of MA-plots in previous Figures. The same color code would be appreciated in Fig 1. Currently, the nuclear mRNAs are turquoise and cytoplasmic mRNAs are orange in Fig 6 (a, d, e and f), but the nuclear/cytoplasmic colors are swapped in Fig 1 as well. Also, all mRNA names are in red color in the MA-plots (b, g, h and i). Matching the nuclear/cytoplasmic colors across figure panels would help the reader to visualize faster the main results.

We have made the suggested color changes.

Reviewer #2:

I thank the authors for addressing my previous comments.

In the response to my question about the advantage of HiVis over existing computational methods, the authors stated and I quote, 'HiVis, by contrast, works on binned data generated by sequencing-based methods such as VisiumHD, Stereo-seq, and Slide-seq, thereby leveraging whole-transcriptome measurements.' However, I did not see examples of the applications of HiVis in Stereo-seq and Slide-seq datasets. I would like to see these demonstrations to be fully convinced that HiVis is a generalizable tool rather than a tool built for just Visium data.

We thank the reviewer for the comment. Indeed, HiVis accepts any dataset that provides an image, a binned expression matrix, and corresponding spatial coordinates, making it compatible with a wide range of technologies beyond VisiumHD.

To demonstrate this, we have now added a new Supplementary Figure S3, "Cross-platform application of HiVis". We imported and analyzed Stereo-seq mouse brain data processed in Qiu et al. 2024 (PMID: 39532097), and showed the results in Fig. S3g-i. We have also implemented a dedicated function for importing these data, along with a usage example, available in the code repository linked in the paper.

In addition, to further demonstrate cross-platform performance on an independent technology, we performed extensive cellular and subcellular analyses on a Xenium dataset from mouse small intestine and show that the resulting localization patterns are highly consistent with those obtained from our VisiumHD analysis (Fig. S3a–f).

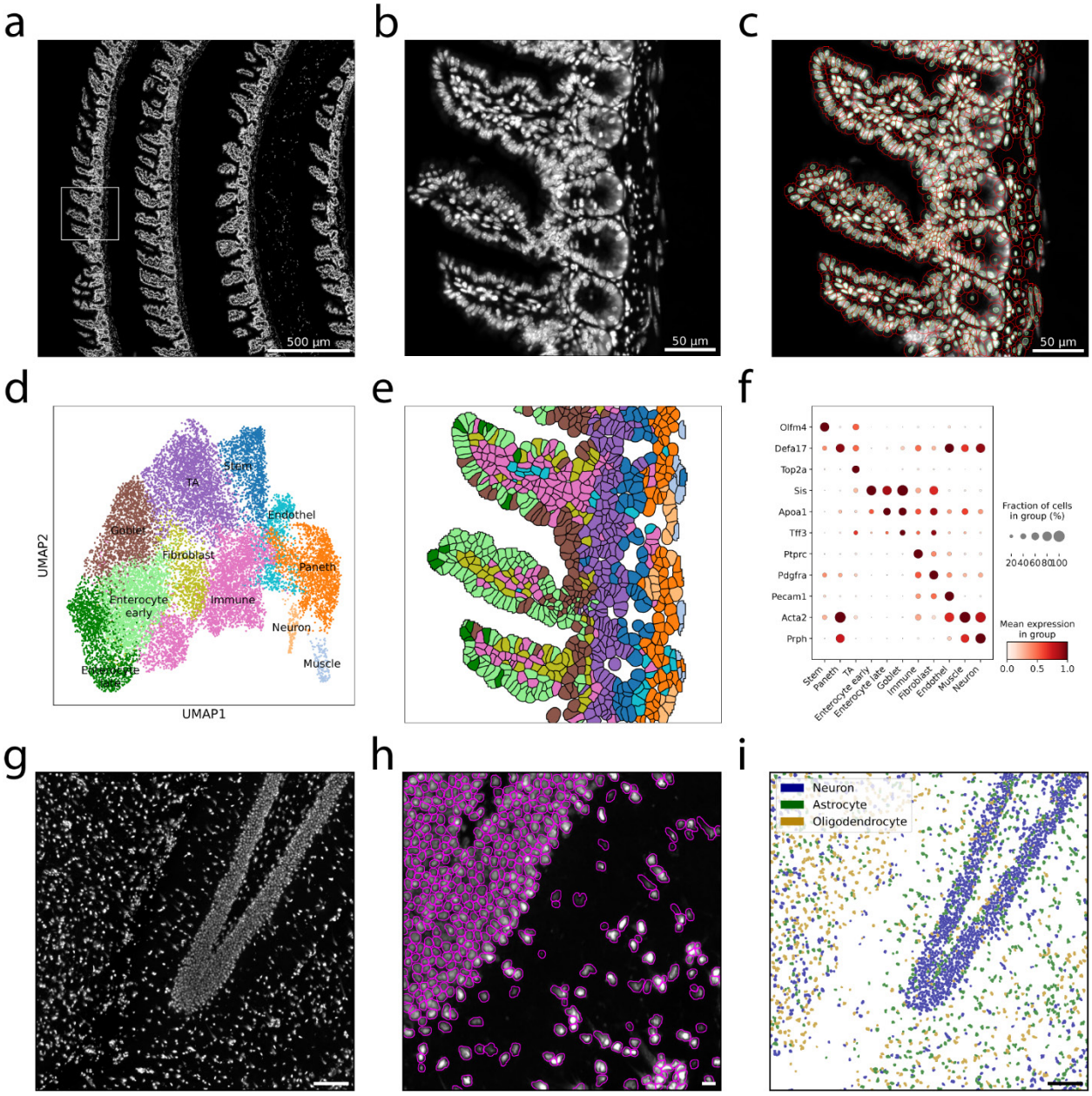

Figure S3 – Cross-platform application of HiVis

(a) *DAPI image of mouse intestine Xenium dataset from Ameku et al. (46). Box denotes selected FOV in (b,c,e). Scalebar 500µm.* ***(b)*** *DAPI image of mouse intestine Xenium dataset, selected FOV. Scalebar 50µm.* ***(c)*** *Same ROI as (b), with single cells segmented in red. Nuclei in green. Scalebar 50µm.* ***(d)*** *Annotated UMAP of single cells colored by cell type.* ***(e)*** *Same FOV as (b), with cells colored by cell type. Colors correspond to the cell-type colors in (d).* ***(f)*** *Dot plot of normalized gene expression for selected markers across cell types.* ***(g)*** *ssDNA image of mouse brain Stereo-seq dataset from Qiu et al. (47). Scalebar 100µm.* ***(h)*** *Single cells segmented in mouse brain Stereo-seq dataset. Scalebar 10µm.* ***(i)*** *Same FOV as (g) with cells colored by cell-type. Scalebar 100µm.*

We also attempted to apply HiVis to Slide-seq datasets; however, Slide-seq does not provide a co-registered tissue image (H&E or fluorescence) linked to the spatial bins. As a result, Slide-seq data lacks the imaging information required for image-based segmentation and feature extraction, which are central to the HiVis framework.

We now clarified the support for other methods with a registered image in the results section on page 3:

"To address this gap, we developed HiVis (HD Integrated Visium Interactive Suite), an interactive, user-friendly, end-to-end platform optimized for 10x VisiumHD datasets, but extended to support other spatial transcriptomics methods that include a registered image (Fig. S1)."

Reviewer #3:

Although the authors made an effort to show that the users can import data from high resolution platforms (MERFISH, Xenium datasets), there is no enough evidence that the tool can analyze those data effectively, especially given that there are existing tools to visualize those data much more efficiently. The additional figure only shows that the tool can display the raw image and very low resolution summary of the transcripts, saying that it is now compatible with multiple platforms is not justified. It is better to acknowledge that it is specialized to Visium HD (which is fine since Visium HD has many properties distinct from imaging based platforms).

We thank the reviewer for the comment. HiVis fully supports other platforms besides VisiumHD. To demonstrate this, we have now added Supplementary Fig. S3 "Cross-platform application of HiVis", which shows the analysis of Xenium dataset with HiVis, including data import and handling, image analysis (nuclear and cell segmentation), compatibility with external tools (Scanpy), and advanced plotting:

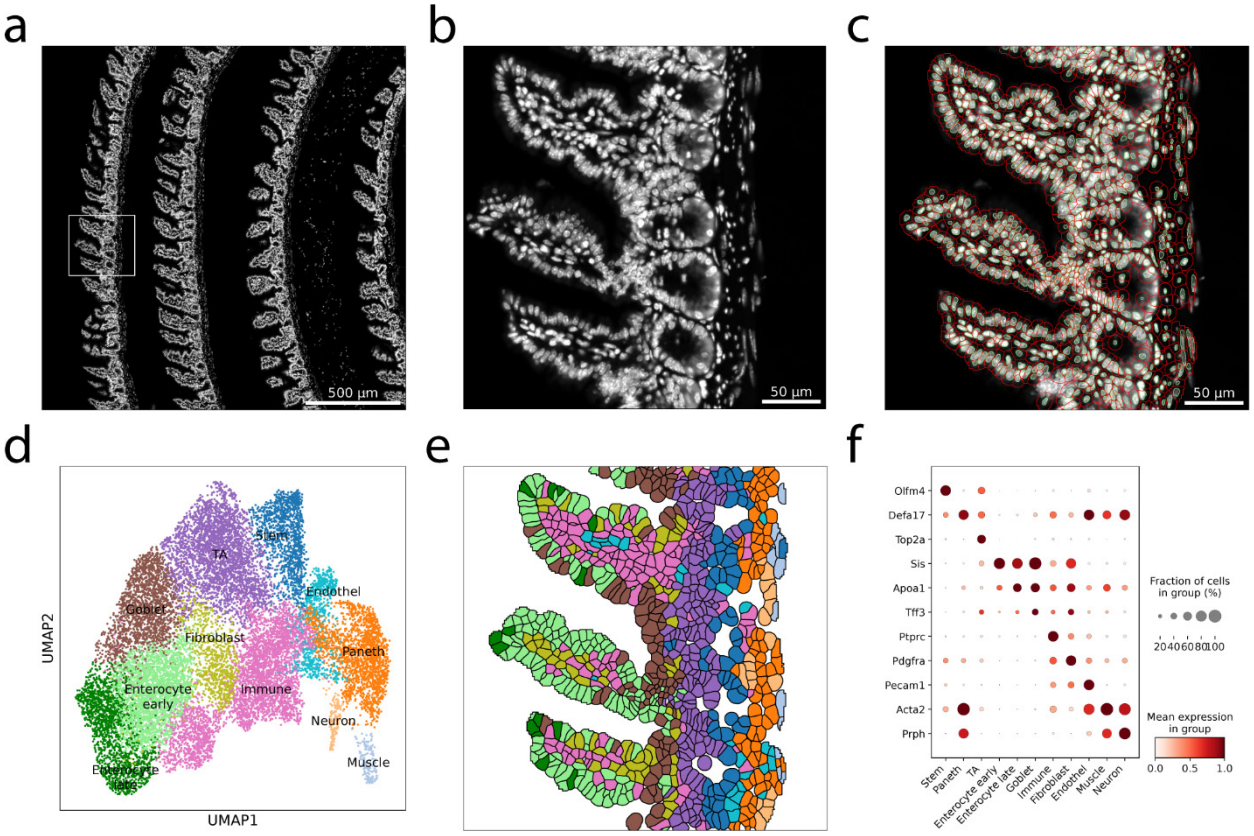

Figure S3 – Analysis of Xenium dataset with HiVis

(a) *DAPI image of mouse intestine Xenium dataset from Ameku et al. (46). Box denotes selected FOV in (b,c,e). Scalebar 500µm.* ***(b)*** *DAPI image of mouse intestine Xenium dataset, selected FOV. Scalebar 50µm.* ***(c)*** *Same ROI as (b), with single cells segmented in red. Nuclei in green. Scalebar 50µm.* ***(d)*** *Annotated UMAP of single cells colored by cell type.* ***(e)*** *Same FOV as (b), with cells colored by cell type. Colors correspond to the cell-type colors in (d).* ***(f)*** *Dot plot of normalized gene expression for selected markers across cell types.*

We describe these results on page 5:

"To further demonstrate the utility of HiVis in extracting spatially resolved single-cell data from image-based platforms beyond VisiumHD, we applied it to a Xenium dataset of the mouse small intestine (46), revealing distinct villus-zonated cellular states (Fig. S3)."

Additionally, we performed a subcellular analysis of the Xenium dataset to assess gene localization. This analysis followed the same workflow used for the VisiumHD data, including data handling, cell and nuclear segmentation, manual annotation, and downstream analyses such as distance measurements and differential gene expression. Using this approach, we identified expected nuclear and cytoplasmic gene

localization patterns (nuclear: *Neat1*, *Vegfa*; cytoplasmic: *Apoa1*, *Fabp2*), which we now show in Fig. S6:

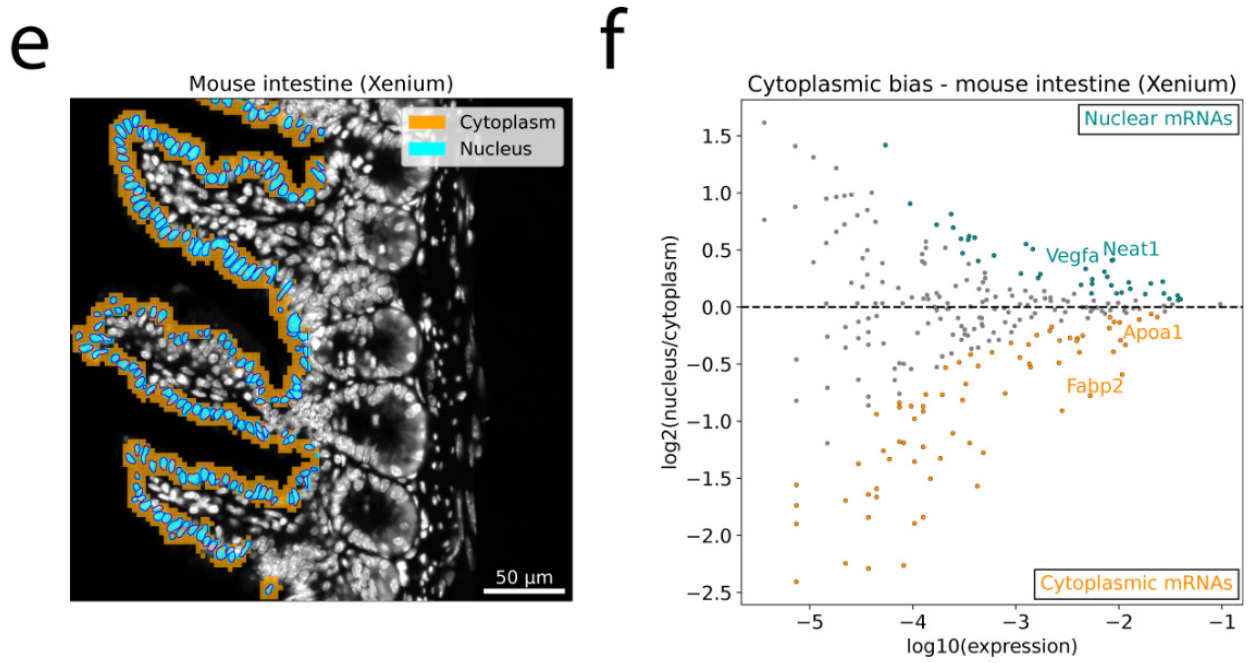

Figure S6 – Mapping nuclear retention in livers and Xenium

(e) *Mouse intestine Xenium DAPI image overlayed with 3×3µm bins colored by nuclear/cytoplasmic assignment, and with nuclear segmentation.* ***(f)*** *MA-plot of differential gene expression results in mouse intestine (Xenium). Significant genes are colored cyan and orange (q<0.1). Selected gene names are shown.*

We describe the results in the text at page 11:

"*We applied similar analysis on published Xenium dataset of mouse small intestine, to demonstrate the compatibility of HiVis with other platforms. We confirmed that nuclear genes such as Neat1 and Vegfa were enriched in the nucleus, while Apoa1 and Fabp2 were enriched in the cytoplasm (Fig. S6e-f).*"

Similarly, we performed an analysis to identify apical and basal genes and found expected apical markers such as *Alpi* and *Apoa1* (Fig. R1). However, because the Xenium panel primarily included stromal genes, limiting broader epithelial interpretation, and because we had already demonstrated the ability of HiVis to analyze Xenium data, we chose not to include this analysis in the manuscript.

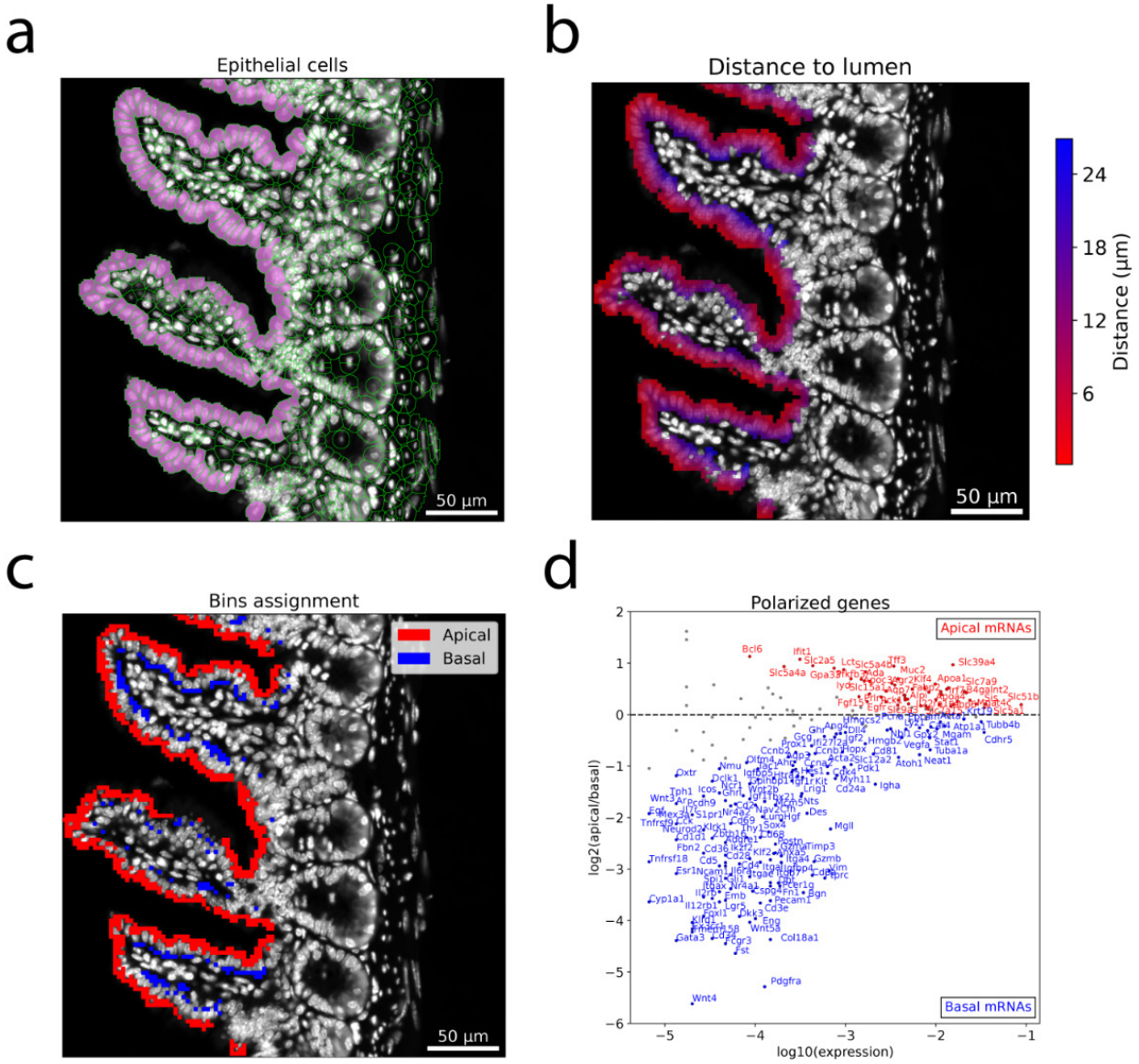

Figure R1 – Mapping apical/basal genes in Xenium dataset

(a) *Mouse intestine Xenium DAPI image, overlayed with segmented cells. Epithelial cells are in pink.* ***(b)*** *Same FOV as (a), overlayed with 3×3µm bins colored by the distance to the lumen.* ***(c)*** *Same FOV as (a), overlayed with 3×3µm bins colored by apical/basal identity, based on distance from lumen inside the epithelial cells.* ***(d)*** *MA-plot of differential gene expression results. Significant genes are colored red and blue (q<0.1). Selected gene names are shown.*

Lastly, to further demonstrate the ability of HiVis to analyze other platforms, we included analysis of Stereo-seq mouse brain dataset (Qiu et al.) in Fig. S3.

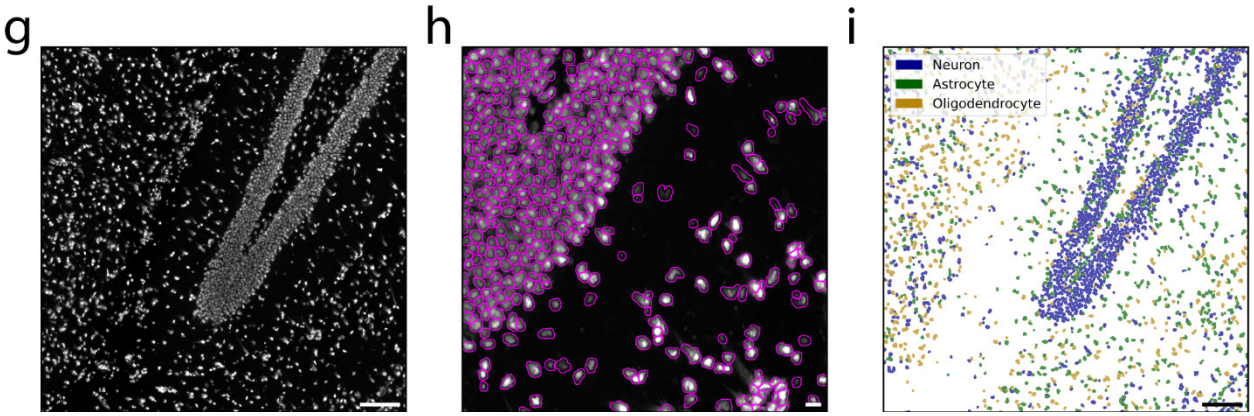

Figure S3 – Cross-platform application of HiVis

(g) *ssDNA image of mouse brain Stereo-seq dataset from Qiu et al. (47). Scalebar 100μm.* ***(h)*** *Single cells segmented in mouse brain Stereo-seq dataset. Scalebar 10μm.* ***(i)*** *Same FOV as (g) with cells colored by cell-type. Scalebar 100μm.*